Experimental Study on the Analysis of the Use of Forward and Rearward Wingtip Fences 90°Cant Angle on Wing Airfoil Eppler 562

Bayu Dwi Cahyo[1,2*], Sutardi[1] and Setyo Hariyadi[1,2]
[1]*Fluid Mechanic Laboratory, Mechanical Engineering Department, FTI, ITS, Surabaya, Indonesia*
[2]*Aviation Polytechnic of Surabaya, Surabaya, Indonesia*

Keywords: Wingtip Fence, Eppler 562, Oil Flow Visualization, C_L/C_D.

Abstract: This research is a detailed experimental study on aerodynamic characteristics for wing model airfoil Eppler 562 with and without wingtip. There are two types of wingtip fences at variations that will be used in this research that are rearward and forward wing tip fence set at cant angle 90°. The chord length of the airfoil is 72 mm and the span length is 300 mm. The Reynolds (Re) number used is 2.3×10^4 (U_∞ = 10 m/s) with angle of attack variations (α) = 0°to 19°. For this research, pressure distributions over the airfoil were measured using a pressure transducer. Moreover, measurements lift and drag forces of the airfoil were obtained by using a load-cell system. Oil flow visualization method was used to represent the surface flow patterns. The experimental results showed that as the angle of attack increased, the separation and the transition points moved towards the leading edge at all models. Furthermore, for airfoil with forward wingtip fence with cant angle 90°C_L/C_D is better than for airfoil with rearward wingtip fence with cant angle 90°and plain wing. Forward wingtip fence showed the best optimum performance of α = 10°settings compared to the other models.

1 INTRODUCTION

The development of aviation technology is currently growing a rapid and promising, especially in the design of aerodynamic forms of aircraft. The outer edge of the wing (wingtip) is one part that has an important role in aircraft. Wingtip design will affect the air flow conditions along the wingspan which will affect the lift coefficient and drag coefficient to improve aerodynamic performance of aircraft(Sutrisno et al., 2015). One important thing to note in the design of a plane is the selection of an airfoil and its modifications. The advantages of the optimal design are a reduction in drag and increasing in lift. The main parameter of wing performance is the C_L/C_D ratio. The wing design is considered good if it has a high value of C_L/C_D ratio. The low value of C_L/C_D ratio is caused by flow separation followed by wake and vortex occurring on wingtip. Flow separation occurs due to excessive adverse pressure gradient (APG) and friction effect. Next, the tip vortex is circular pattern of air flows from below the wing to the top of the wing around the wingtip. Separation and vortex are two phenomena that increase drag component and reduce lift due to reduce the wingspan effectiveness. One attempt to reduce the vortex is delaying the separation. Another attempt is wingtip modifications by addition of winglet.

Turanoguz and Alemdaroglu (2015) performed a numerical simulation on airfoil type Eppler 562 by varying winglet in the form of shifted downstream type wingtip, hoerner type wingtip, and blended type wingtip. In the research, it was showed that the winglet was able to increase the C_L/C_D value. Myilsamy et al. (2015) et al conducted numerical investigation on NACA 4412 airfoil coordinates for the wing design and the winglet with the blended design. The design of the entire wing including winglet were examined at different cant angles of winglets varying from 0°, 30°and 90°degrees at different angles of attack from -2°to 10°. They have observed among the cases of this study, wings with winglets produces higher C_L/C_D ratio performance than the normal aircraft wing without winglets.

Suranto Putro et al. (2016) investigated by numerical simulation on airfoil type NACA 43018 by affixing winglet in the form of forward wingtip fence and rearward wingtip fence. In the study it was showed that the addition of winglet was able to increase the C_L/C_D value up to 22.9% for forward wingtip fence type at α = 2°. Ristic (2007) studied experimentally on NACA2415 airfoil by varying angle of attack from

Cahyo, B., , S. and Hariyadi, S.
Experimental Study on the Analysis of the Use of Forward and Rearward Wingtip Fences 90o Cant Angle on Wing Airfoil Eppler 562.
DOI: 10.5220/0008549102060214
In *Proceedings of the 3rd International Conference on Marine Technology (SENTA 2018)*, pages 206-214
ISBN: 978-989-758-436-7

-12°to 20°at low Reynolds. In this study, the flow visualizations were done by using oil flow technique for qualitative analysis of the transition zone. The experimental results showed that as the angle of attack increased, the separation and the transition points moved towards the leading edge at all Reynolds numbers.

The aim of this study is to evaluate aerodynamic performance of airfoil Eppler 562 (E562) without and with the addition of wingtip fence. There are two types of wingtip fence variations that will be used in this research. They are rearward wing tip fence and forward wing tip fence with cant angle 90°The Reynolds (Re) number used is 2.3 $\times$ 104 (U_∞ = 10 m/s) with angle of attack variations (α) = 0°, 2°, 4°, 6°, 8°, 10°, 12°, 15°, 17°and 19°.

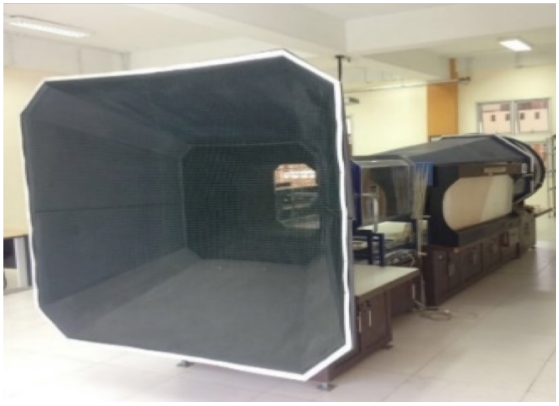

Figure 1: Wind Tunnel WT-60 Set-up

Figure 2: Schematic Diagram of The Experimental Set-up.

2 RESEARCH METHODOLOGY

2.1 Wind Tunnel and Models

Experiments were conducted in the Aerodynamics Laboratory Department of Aircraft Engineering at Aviation Polytechnic of Surabaya The experiments were carried out in a low-speed, suction-type wind tunnel with a square test section dimension of 600 mm $\times$ 600 mm. The ratio of cross sectional area of contraction cone was $\pm$ 9:1 and the side walls of the working section were expanded with a divergence angle of 0.3°on each side to minimize boundary layer effects on the working section walls, and to give a constant static pressure. The wind tunnel could be operated at a maximum air speed of 50 m/s. The experiments were carried out at Reynolds (*Re*) numbers of 2.3 $\times$ 104 based on chord length of airfoil (c) and free-stream velocity ($U\infty$). The experimental setup and schematic diagram are shown in Figure 1 and 2.

The airfoil models were manufactured out of acrylic sheet (Figure 3) that was formed according to airfoil Eppler 562 profile performed by heated. The manufactured airfoils have a span length of 300 mm, and a chord length of c= 72 mm. The profile winglet maximum chord forward wingtip fence from leading edge and winglet maximum chord rearward wingtip fence from leading edge are 72 mm and 22.62 mm respectively, and the winglet minimum chord is 15.12 mm.

2.2 Pressure Measurements

For the measurement of pressure distributions of suction and pressure surfaces on the Eppler 562 airfoil, a system including a pitot-static tube, a National Instrument unit, a 32 channel pressure transducer and 32 pressure tapping of 1/16 inch in diameter, which are flush along the mid-span and tip-span alternately of the upper and lower surfaces of the wing was used (Figure 4). Pressure measurements were carried out by using a computer data acquisition system. The pressure was measured by using ni cdaq-9172 National Instrument which the output was a voltage. The maximum response time of the pressure transducer was about 1 ms. Pressure signals were obtained at a sampling rate of 100 samples data per second or in one snapshot and a Signal Express software from Ni-max was used to display the results of conversion analog pressure data to digital (A/D) in ASCI format data, and final post-processing was complemented in Microsoft Excel Software to calculate the mean pressure distributions and created the graph. Experiments were investigated over a range of angles of attack in order to calculate the pressure coefficient distribution on all type airfoil.

2.3 Force Measurements

An external load-cell system was used for measuring the lift and drag forces on the airfoil. The Eagle Tree system data recorder (Figure 5) software used to display data from DAQ system that converted an analog input to digital output of the lift and drag forces

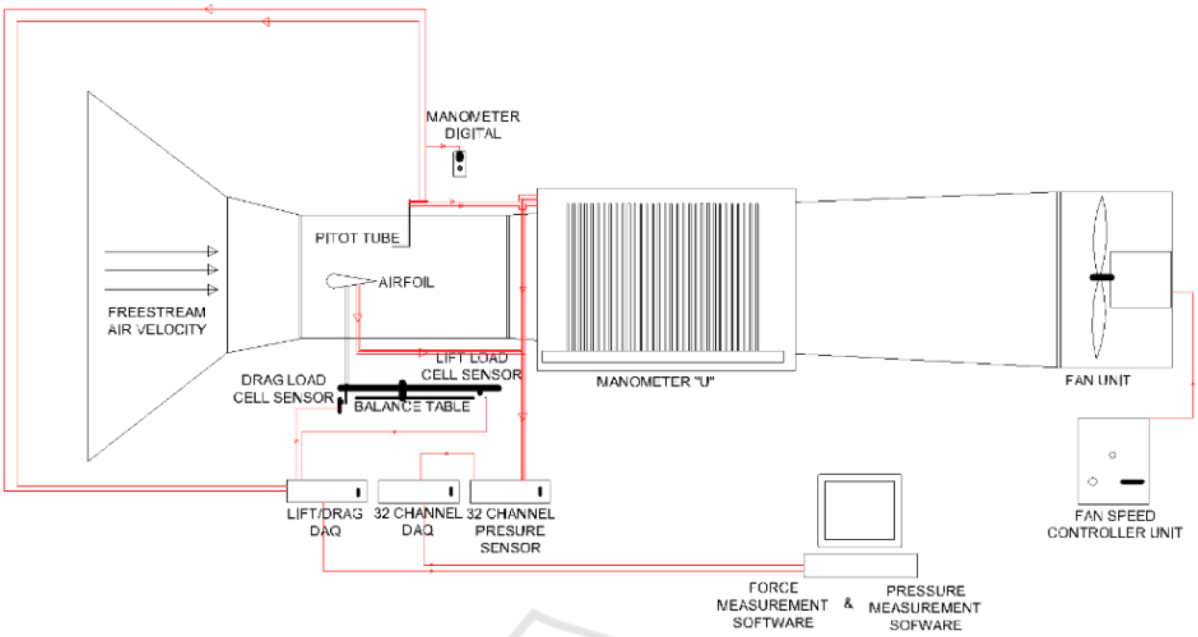

Figure 3: Airfoil models manufactured with end-plate: a) plain wing b) rearward wingtip fence and c) forward wingtip fence.

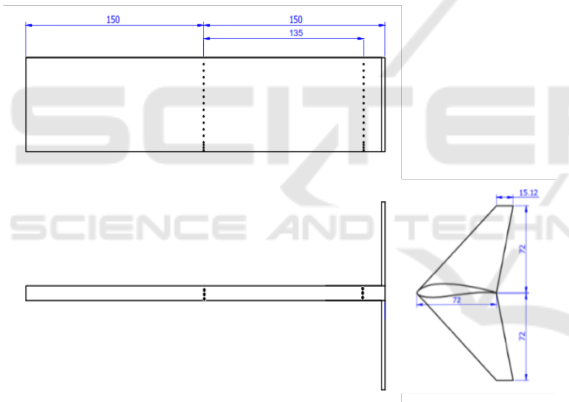

Figure 4: Pressure Tap Location on Midspan and Tip Span at All Models.

Figure 5: Experimental Set-up for The Force Measurements.

in gram. The calibration was performed by loading the load cell with known weights. Calibration was repeated before each set of experiments to ensure consistency. Sets of data chosen at random were repeated. The force data was collected at a sampling 100 samples data over 120 s in FDR format data. Mean forces and its coefficients were calculated using Microsoft Excel Software.

2.4 Oil Flow Visualization

The simple and effective way of observing surface flow events was used oil flow visualization(Ristic, 2007). This method performed on the mat black airfoil surface was painted before with pigmented oil was used to get the clear photograph of surface flow events (Figure 6) and the wind tunnel is run. It is important that the type of oil mixture which would work at the speed of the wind tunnel. The mix should have the right consistency to effectively indicate the development of the boundary layer. The simplest mix to make was palm oil and titanium dioxide (TiO_2) the ratio of palm oil to titanium dioxide was roughly 5:1 then stir for 15 minutes until the TiO_2 fine granules not visible. Furthermore, the mixture was diluted by adding kerosene the ratio 5:1, respectively. And this ratio of mixture was used in the present study (Figure

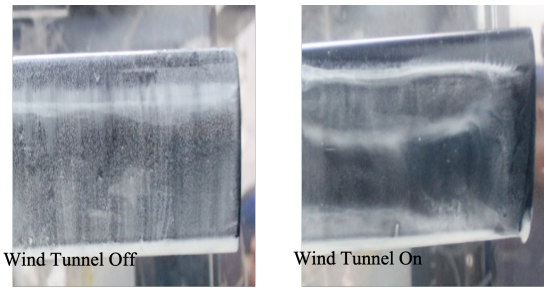

Figure 6: Sample of Oil-flow Visualization Experiment over Eppler 562 Aerofoil on which Oil laid.

6). However, the pigment was added in some doses based on Reynolds number.

3 RESULTS AND DISCUSSIONS

3.1 Drag Coefficient (C_D)

The nature of the air which always moves from high pressure to lower pressure towards the tip of the wing, causes movement of air from lower side wing which is directed outward around the outer edge of the wing such as "spill" and created a vortex around the wingtip. The existence of vortex will disrupt the air flow along the wing thereby reducing the effective area of the wing which resulted in an increase in drag. This leads to a decrease in the average attack angle relative to the airflow around the wing, too. The coefficient of lift and the coefficient of drag have been calculated from the experimental results. Also various graphs have been drawn to examine the measured and calculated data nature.

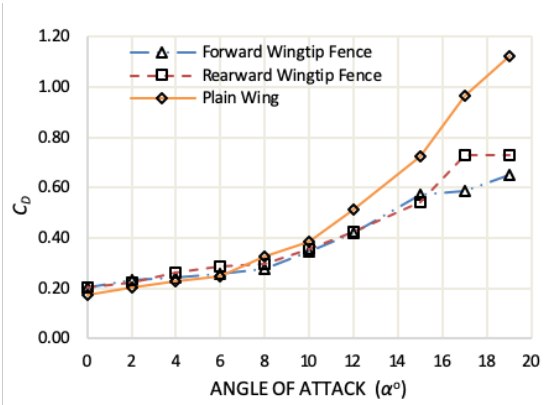

Figure 7: Drag Coefficient (C_D) vs α on Plain Airfoil and using Winglet.

In Figure 7, it is shown that the drag coefficient all of the aircraft wing model under test. The drag increases slowly with increase in angle of attack to a certain value and then it increases rapidly with further increase in angle of attack. The initial value of drag coefficient of the plain wing at zero angle of attack for Reynolds number 2.3×10^4 is 0.1713. The value of the drag coefficient at the transition point i.e. at an angle of attack of 8°is 0.3271. The experiments have been done up to an angle of attack of 19°. At the maximum angle of attack of 19°the drag coefficient is 1.1216. The rapid increase in drag coefficient, which occurs at higher values of angle of attack, is probably due to the increasing region of separated flow over the wing surface, which creates a large pressure drag. The comparison drag coefficient data for wingtip for the three variations i.e. plain wing (without wingtip), rearward wingtip fence cant angle 90°, and forward wingtip fence cant angle 90°are given in Fig.7. For all wingtip variations, a similar pattern has been observed. At 10°angle of attack the drag coefficients for the plain (without wingtip), rearward wingtip fence cant angle 90°, and forward wingtip fence cant angle 90°are 0.3832, 0.3561, and 0.3468 respectively, and began to effectively reduce the drag. It appears that drag coefficient using forward wingtip fence is lowest than the other models.

3.2 Lift Coefficient (C_L

In Figure 8, it is shown that the lift coefficient all of the aircraft wing model under test. The lift increases with increase in angle of attack to a maximum value and thereby decreases with further increase in angle of attack. The initial value of lift coefficient of the plain wing at zero angle of attack for a chord based Reynolds number 2.3×10^4 is 0.2897. The maximum value of the lift coefficient is 1.542 and this maximum values occur at an angle of attack of 12°. The experiments have been done up to an angle of attack of 19°. At the maximum angle of attack of 19°the lift coefficient is 0.5452. The reason for a drop in lift coefficient beyond a certain angle of attack e.g. 12°is probably due to the flow separation, which occurs over the wing surface instead of having a streamlined laminar flow there. This condition is called stalling condition and the corresponding angle of attack is called stalling angle. The stalling angle occurs to be 12°. The comparison maximum lift coefficient data for wingtip for the three variations: plain wing (without wingtip), rearward wingtip fence cant angle 90°, and forward wingtip fence cant angle 90°are given in Figure 8. are 0.6075, 0.7277 and 0.8423 respectively corresponding to an angle of attack of 12°, 17°, and 17°respectively which is also the stall angle of attack. The addition of the winglet

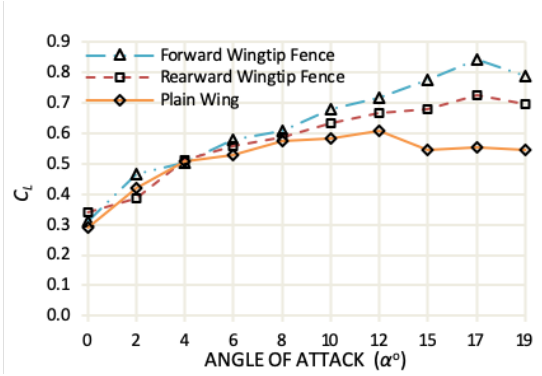

Figure 8: Lift Coefficient (C_L) vs α on Plain Airfoil and using Winglet.

effective enough to prevent air rotation (vortex) on the wingtips caused by the encounter of the lower air of the high pressure wing with low pressure upper air wing which reduces the angle of attack effectively. From the graph, it can be concluded that lift coefficient for using forward wingtip fence is highest than the other variations and it is also seen that the use of wingtip fence can delay the occurrence of stalls.

3.3 Lift and Drag Coefficient (C_L/C_D)

A winglet's main purpose is to improve performance by reducing drag. By using the winglet, the strength of the vortex can be reduced and the induced drag can also be reduced. Such performance improvements can be seen in the C_L/C_D comparison graph. The C_L/C_D ratio is the outcome of the observations made in the two preceding sections. It is observed from the Fig. 9 that the C_L/C_D ratio for all the configurations considered increases with an angle of attack to its maximum value and thereby it decreases with further increase in angle of attack. As the effective area of the wing increased, the value of the C_L/C_D get in increased. Vortex tips derived from the lower side wings contribute to reducing this effective area and also increase the induced drag of the wing. If the winglet can prevent or minimize air spill effectively, it can reduce tip vortex.

Table 1: The Separation Point (X_s) vs x/c obtained from The Results of The Oil-flow Visualization.

Re Number	α°	X_s Plain	X_s Rearward Wingtip Fence	X_s Forward Wingtip Fence
2.3 x 104	0	0.1	0.1	0.1
	4	0.08	0.03	0.03
	8	0.03	0.02	0.02
	12	0.01	0.01	0.01

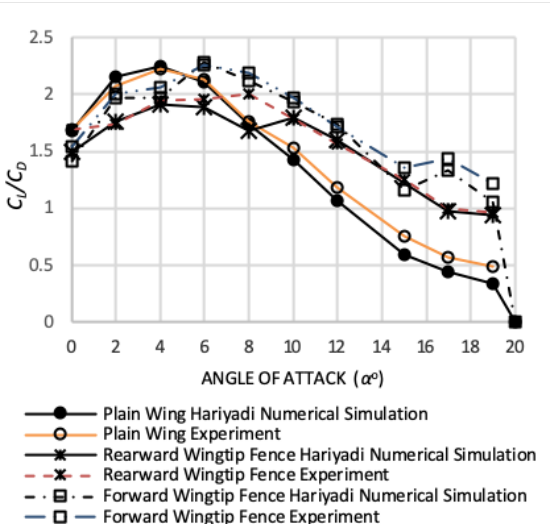

Figure 9: Comparison of C_L/C_D between Plain Airfoil and Airfoil with Addition of Winglet from Experimental Result.

Figure 9 shows comparison of C_L/C_D ratio on plain wing and with variations winglet in some angle of attack. This indicates that with the addition of winglet will increase the C_L/C_D ratio and show an improve trend along with the increase of angle of attack. The airfoil wing model without winglet gives a measured C_L/C_D ratio of 1.762 whereas the respective values of the C_L/C_D ratio for rearward wingtip fence cant angle 90°, and forward wingtip fence cant angle 90°are 2.00, and 2.188 respectively at an angle of attack of 8°.

Practically it is observed that the C_L/C_D ratio versus angle of attack curve gives similar results for 8 to 15 degrees, for the all type of without and with winglet. It can be said that the wing with forward wingtip fence cant angle 90°variation has the better performance as compared to plain wing (without wingtip) and rearward wingtip fence cant angle 90°and it is giving the better C_L/C_D ratio (2.188). It also shown that the result of experimentally have quite good agreement with Suranto Putro et al. (2018) numerical research did. The graph indicated as the angle of attack increase, the trend C_L/C_D experimentally have a similar to numerical simulation.

3.4 Pressure Coefficient (C_P)

The pressure coefficients were calculated from the pressure readings of Signal Express software that obtained from the pressure tapping at many points across the midspan and tip span airfoil surface. Figure 10 describes the evolution of the pressure coefficient as the angle of attack were increased, the graphs of pressure distribution (C_P) over the Eppler 562 airfoil plain

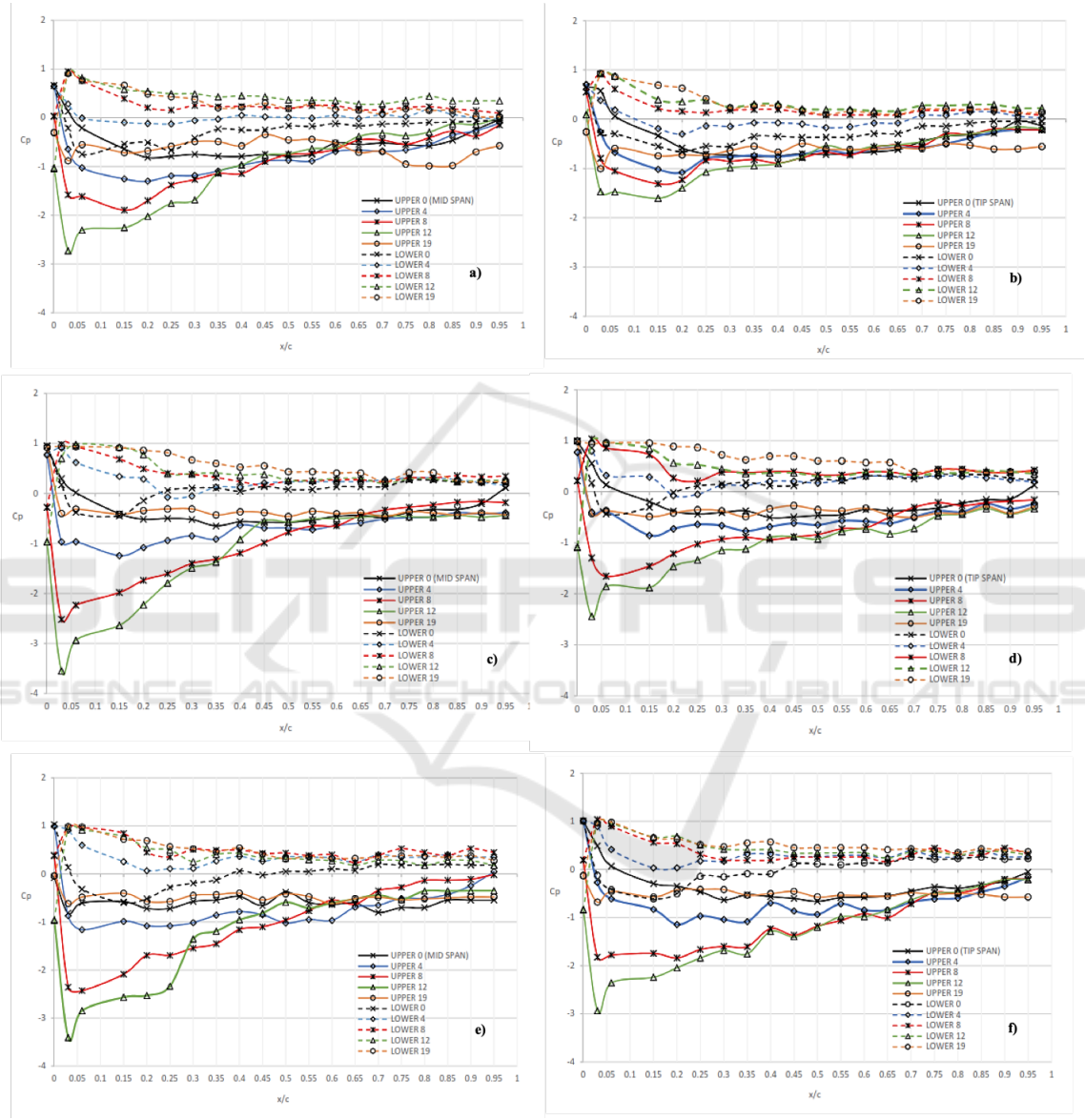

Figure 10: Pressure coefficient (C_P) versus the angle of attack (α) 0°to 19°at pressure tap location: a) plain wing mid span b) plain wing tip span c) rearward wingtip fence mid span d) rearward wingtip fence tip span e) forward wingtip fence mid span f) forward wingtip fence tip span.

wing and with variations of winglet at angles of α = 0°, 4°, 8°, 12°, 19°at Re = 2.3 $\times$ 10^4. In general these plots illustrate the development of the boundary layer as the pressure slowly increases after peak suction from the leading-edge to the trailing-edge. Figure 10a shows at the plain wing (without winglet) that the effective midspan better than tip span area. This can be known that the resulting plot pressure coefficient magnitude at midspan is wider than tip-span area at all condition of angle of attack. This indicates that tip vortex affecting characteristics air flow at the wingtip area, while midspan area not affected because it was longer distance from the wingtip.

Figures 10c and 10e are airfoil with adding rearward wingtip fence cant angle 90°, and forward wingtip fence cant angle 90°, respectively. It can be seen that forward wingtip fence has a bigger area pressure coefficient distribution than rearward wingtip fence. This condition is caused by tip on rearward wingtip fence model not completely cover by the endplate. So, there is still an air spill from lower side disrupts effective air flow on upper side especially in the leading edge wingtip area. Consequently, wing performance at rearward wingtip fence types worse than forward wingtip fence ones.

3.5 Oil Flow Visualization Results

In Figures 11 and 12, it is describes the concept boundary layer separation process, oil flow visualization was applied to the upper surface of the airfoil at angles of attack of 0°, 4°, 8°, and 12°. The dense area of pigment describes the flow has decelerated, it means the point at which the pressure gradient repeal causing separation.

As the angle of attack increases the separation point moves towards the leading edge at all four angle of attack that the vorticity magnitude of the vortex will increase as the angle of attack increases. At angle of attack 0°(Fig. 11a) this occurs at 10% chord, 4°(Figure 12d) at 8% chord, 8°(Figure 13a) at 3% chord and for 12°(Figure 12d) at 1% chord. Furthermore, the separation point (X_s) vs x/c obtained from the results of the oil-flow visualization and pressure coefficient experiments can be seen in Table 1. It also seen tip vortex get in interference at upper side wingtip has an impact to coefficient of lift. The higher the angle of attack the vortex is formed the wider. As the vortex formation area increase the lift coefficient will be decrease. In Fig. 12 shows vortex formation of the tip where plain wing produces widest vortex contour.

The forward wingtip fence produces smallest vortex contour than other types. It was occurs due to the vortex formation of the tip is obstructed by the tip of the winglet. Therefore, design endplate cover tip from front until rear of the tip causes tendency of airflow from the lower surface near the end of the wing to "jump" to the upper surface can be effectively reduced. As the disruption of airflow from lower surface decrease the vortex formation area will decrease. It follow the rising of lift coefficient.

4 CONCLUSIONS

The results of this experimental investigation show that the use of winglet can improve the performance on airfoils Eppler 562 using variations of wingtip fence will increase drag along with increasing angle of attack. However, with the addition of winglet, lift force can be improved better than plain wing. Winglet causes the formation of vortex tip can be reduced significantly.

From the experimental study it was concluded that the use of winglet can produce some flow characteristics, namely:

- Increased angle of attack will increase wingtip vortices and drag coefficient.
- Wing with the addition of forward wingtip fence cant angel 90°produces C_L/C_D higher than plain wing and rearward wingtip fence cant angel 90°.
- To produce a high C_L/C_D then the pressure required on the lower surface is much higher than the upper surface. Forward wingtip fence cant angel 90°produces better C_L/C_D than rearward wingtip fence cant angel 90°because forward wingtip fence enlarges the formation of effective area so that the lift can be increased. It is generally found that the addition of forward wingtip fence reduces the induced drag than plain wing.
- On forward wingtip fence cant angel 90°produce higher performance than other wing start at α = 6°while rearward wingtip fence cant angel 90°produce better performance start at α = 8°.
- In the oil-flow visualization and pressure distribution experiments, it was concluded that as the angle of attack increased the separation point moves towards the leading edge at wing airfoil Eppler 562 without and with winglet.
- Forward wingtip fence cant angle produce smallest vortex formation area at tip than other types that performed by oil-flow visualization.

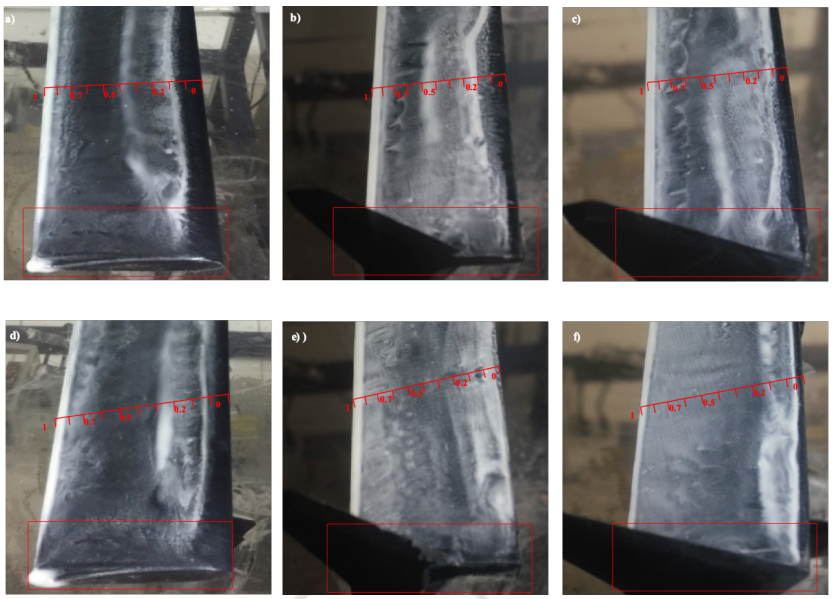

Figure 11: The photographs of oil-flow visualization experiments over the Eppler 562 airfoil for $\alpha = 0^{\circ}$ (a) plain wing (b) rearward wingtip fence (c) forward wingtip fence, for $\alpha = 4^{\circ}$ (a) plain wing (b) rearward wingtip fence (c) forward wingtip fence.

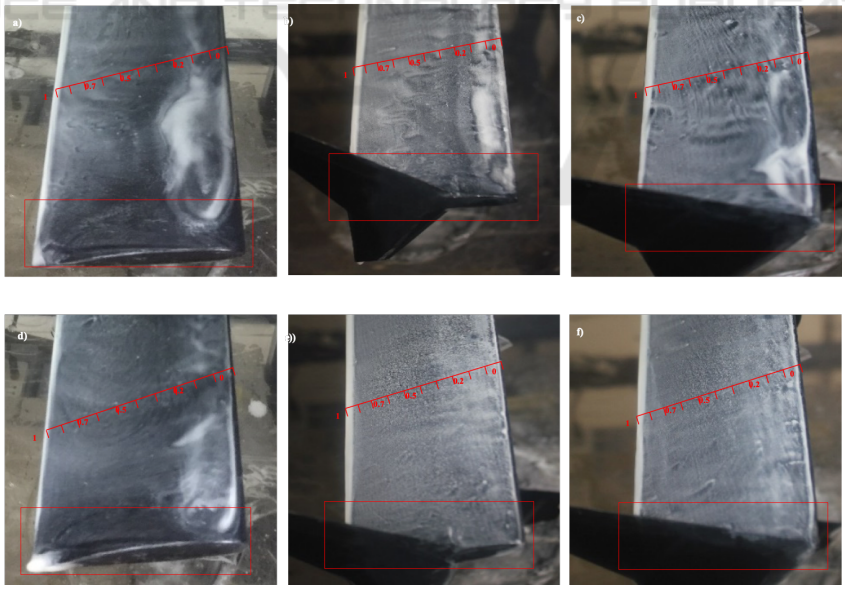

Figure 12: The photographs of oil-flow visualization experiments over the Eppler 562 airfoil for $\alpha = 8^{\circ}$ (a) plain wing (b) rearward wingtip fence (c) forward wingtip fence, for $\alpha = 12^{\circ}$ (a) plain wing (b) rearward wingtip fence (c) forward wingtip fence.

REFERENCES

Myilsamy, D., Thirumalai, Y., and P S, P. (2015). Performance investigation of an aircraft wing at various cant angles of winglets using cfd simulation.

Ristic, S. (2007). Flow visualisation techniques in wind tunnels part i – non optical methods. *Scientific Technical Review LVII N.*, 1.

Suranto Putro, S., Sutardi, S., and Widodo, W. (2016). Numerical study of aerodynamic analysis on wing airfoil naca 43018 with the addition of forward and rearward wingtip fence. volume 1778.

Suranto Putro, S., Sutardi, S., and Widodo, W. (2018). Drag reduction analysis of wing airfoil e562 with forward wingtip fence at cant angle variations of 75° and 90°. volume 2001, page 050003.

Sutrisno, T., Mirmanto, H., Sasongko, H., and Noor, D. (2015). Study of the secondary flow structures caused the addition forward facing step turbulence generated: Case study: Horseshoe vortex between 9c7/32.5c50 body and endwall. *Advances and Applications in Fluid Mechanics*, 18:129–144.

Turanoguz, E. and Alemdaroglu, N. (2015). Design of a medium range tactical uav and improvement of its performance by using winglets. pages 1074–1083.